## ORIGINAL RESEARCH

Adipokine C1q/Tumor Necrosis Factor- Related Protein 3 (CTRP3) Attenuates Intestinal Inflammation Via Sirtuin 1/NF-κB Signaling

Huimin Yu,[1] Zixin Zhang,[1] Gangping Li,[1,*] Yan Feng,[2] Lingling Xian,[3,§] Fatemeh Bakhsh,[4] Dongqing Xu,[5] Cheng Xu,[6] Tyrus Vong,[1] Bin Wu,[4] Florin M. Selaru,[1] Fengyi Wan,[5] Mark Donowitz,[1,6] and G. William Wong[6]

[1]Division of Gastroenterology and Hepatology, Department of Medicine, Johns Hopkins University School of Medicine, Baltimore, Maryland; [2]Department of Pathology and Laboratory Medicine, Pennsylvania Hospital, Penn Medicine, Philadelphia, Pennsylvania; [3]Division of Hematology, Department of Medicine, Johns Hopkins University School of Medicine, Baltimore, Maryland; [4]Department of Biophysics and Biophysics and Biochemistry, Johns Hopkins University School of Medicine, Baltimore, Maryland; [5]Department of Biochemistry and Molecular Biology, Bloomberg School of Public Health, Johns Hopkins University, Baltimore, Maryland; and [6]Department of Physiology, Johns Hopkins University School of Medicine, Baltimore, Maryland
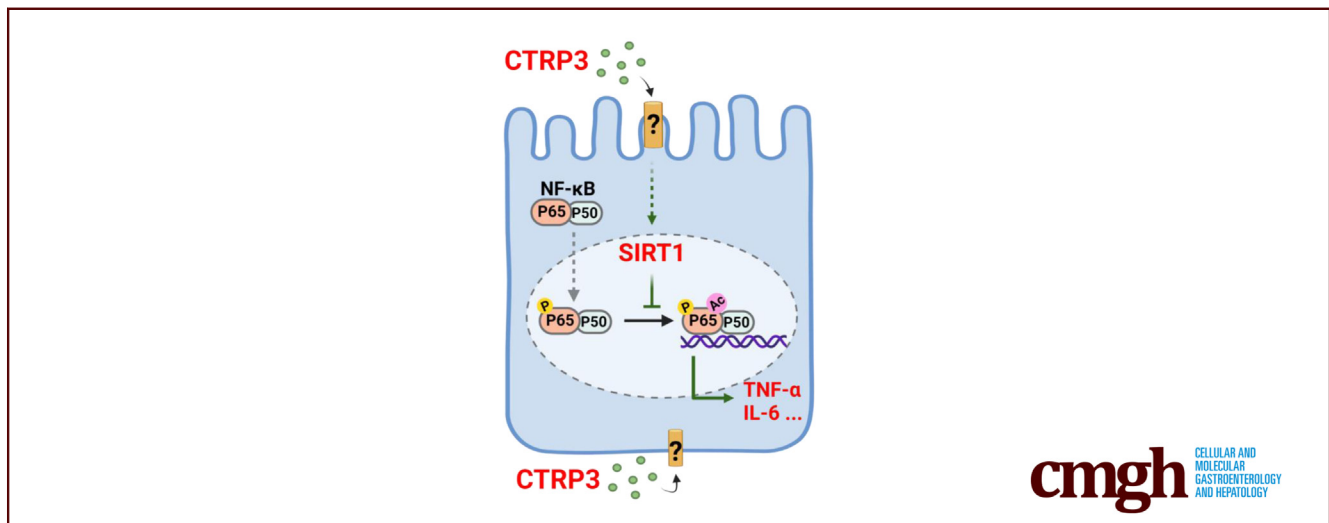
SUMMARY

Here, we report that CTRP3 exerts its anti-inflammatory effect on intestinal inflammation through SIRT1/NF-κB signaling by using *in vivo* complementary KO and Tg mouse colitis models and *ex vivo* intestinal organoid cultures. In patients with IBD, reduced CTRP3 expression in the intestinal mucosa correlated with reduced SIRT1 and increased NF-κB activation and proinflammatory cytokines.

BACKGROUND & AIMS: The adipokine CTRP3 has anti-inflammatory effects in several nonintestinal disorders. Although serum CTRP3 is reduced in patients with inflammatory bowel disease (IBD), its function in IBD has not been established. Here, we elucidate the function of CTRP3 in intestinal inflammation.

METHODS: CTRP3 knockout (KO) and overexpressing transgenic (Tg) mice, along with their corresponding wild-type littermates, were treated with dextran sulfate sodium for 6–10 days. Colitis phenotypes and histologic data were analyzed. CTRP3-mediated signaling was examined in murine and human intestinal mucosa and mouse intestinal organoids derived from CTRP3 KO and Tg mice.

RESULTS: CTRP3 KO mice developed more severe colitis, whereas CTRP3 Tg mice developed less severe colitis than wild-type littermates. The deletion of CTRP3 correlated with decreased levels of Sirtuin-1 (SIRT1), a histone deacetylase, and increased levels of phosphorylated/acetylated NF-κB subunit p65 and proinflammatory cytokines tumor necrosis factor-α and interleukin-6. Results from CTRP3 Tg mice were inverse to those from CTRP3 KO mice. The addition of SIRT1 activator resveratrol to KO intestinal organoids and SIRT1 inhibitor Ex-527 to Tg intestinal organoids suggest that SIRT1 is a downstream effector of CTRP3-related inflammatory changes. In patients with IBD, a similar CTRP3/SIRT1/NF-κB relationship was observed.

CONCLUSIONS: CTRP3 expression levels correlate negatively with intestinal inflammation in acute mouse colitis models and

patients with IBD. CTRP3 may attenuate intestinal inflammation via SIRT1/NF-κB signaling. The manipulation of CTRP3 signaling, including through the use of SIRT1 activators, may offer translational potential in the treatment of IBD. (Cell Mol Gastroenterol Hepatol 2023;15:1000–1015; https://doi.org/10.1016/j.jcmgh.2022.12.013)

Keywords: Adipokine CTRP3; Intestinal Inflammation; IBD; SIRT1/NF-κB Signaling; Intestinal organoids.

Inflammatory bowel disease (IBD), including Crohn's disease (CD) and ulcerative colitis (UC), is a chronic, debilitating inflammatory disorder of the gastrointestinal tract that affects 3 million people in the United States.[1-3] Despite recent advances in biologics (most notably the advent of tumor necrosis factor [TNF]-α inhibitors), nearly one-third of patients with IBD fail to respond to existing therapies.[4-7] There is a pressing need to develop evidence-based, novel strategies to control refractory inflammation in IBD.

The complex interplay between mesenteric fat and intestinal inflammation in IBD has drawn interest since Drs Crohn and Otani first recognized the presence of hyperplastic mesenteric fat wrapped around the inflamed intestine as an indicator of severe disease.[8-10] Despite the recognized association of this "creeping fat" with disease progression, the pathogenetic function of mesenteric fat and adipokines in IBD remains obscure.[11-15] Mesenteric fat is one of the sources of adipokines and cytokines responsible for inflammatory processes associated with IBD.[16-18] And yet it also seems to have modulatory effects, serving as a barrier to inflammation and controlling immune responses to translocated gut bacteria.[19]

Among the mediators secreted by mesenteric fat, C1q/TNF-Related Protein 3 (CTRP3), is of particular interest.[20-23] First characterized in 2004, CTRP3 contains a C1q globular domain similar to adiponectin and TNF, both of which are known to be involved in intestinal inflammation.[24-30] In obesity, type 2 diabetes, and metabolic syndrome, reduced CTRP3 level has been found to correlate negatively with levels of several proinflammatory cytokines, including TNF-α, interleukin (IL)-6, IL-8, and C-reactive protein.[31-35] Several human studies have shown reduced CTRP3 levels in obesity[29,33,34,36,37] and diabetes.[29,31,32,38] A recent study reported that patients with IBD had lower serum CTRP3 levels.[39] To date, however, the function of CTRP3 in IBD has not been established.

Although no CTRP3 receptors have been identified,[40] CTRP3 has been linked to a variety of downstream signaling pathways.[21,29] Recent murine studies using an adenovirus-mediated delivery system to overexpress CTRP3 suggest that CTRP3 may activate histone deacetylase sirtuin-1 (SIRT1) to exert protective effects in acute pancreatitis,[41] collagen-induced arthritis,[42] and cardiac inflammation.[43,44] SIRT1 is a known key repressor of intestinal inflammation in IBD. Specifically, it is thought to suppress phosphorylation and acetylation of the nuclear factor (NF)-κB p65 subunit and thereby reduce expression of the proinflammatory cytokines TNF-α and IL-6.[45-47] In the serum and intestinal tissue of patients with IBD and mice with dextran sulfate

sodium (DSS)-induced colitis, SIRT1 levels are reduced.[48-50] Thus, we hypothesized that CTRP3 suppresses intestinal inflammation via SIRT1/NF-κB signaling.

To test this hypothesis, we first generated acute DSS-induced colitis models in complementary CTRP3 knockout (KO) and overexpressing transgenic (Tg) mice and demonstrated that CTRP3 expression levels correlate negatively with intestinal inflammation. Second, we found that CTRP3 levels correlate positively with SIRT1 and negatively with phosphorylation and acetylation of NF-κB p65 and proinflammatory cytokines TNF-α and IL-6 in acute colitis models of CTRP3 KO and Tg mice. Third, we added SIRT1 activator resveratrol to KO intestinal organoids and SIRT1 inhibitor Ex-527 to Tg intestinal organoids and established that the SIRT1 accounted for the downstream, anti-inflammatory effects of CTRP3. Fourth, we found a similar CTRP3/SIRT1/NF-κB relationship in the intestinal mucosa of patients with UC and CD. Using in vivo complementary CTRP3 KO and Tg mouse colitis models, ex vivo mouse intestinal organoid cultures, and intestinal mucosa from patients with IBD, we link CTRP3 to a reduction in intestinal inflammation via SIRT1/NF-κB signaling and raise the possibility that CTRP3 protein and/or SIRT1 activators may represent a novel drug target for IBD. More broadly, our findings add to the growing understanding of the role of adipokines in IBD pathogenesis, and may assist in the development of new, adipokine-based treatments for IBD.

Results
Expression of CTRP3 in Intestinal Tissue and Attached Mesenteric Fat

We conducted immunofluorescence staining of full-thickness sections of wild-type (WT) mouse colonic tissue and found that CTRP3 protein was expressed in intestinal epithelial cells, intestinal smooth muscle cells, and attached mesenteric fat (Figure 1A). Single-molecule RNA fluorescence in situ hybridization of WT mouse colonic tissue confirmed CTRP3 mRNA expression in all 3 cell types (Figure 1B). Colonic tissue from CTRP3 KO mice was used as a negative control in both experiments (data not shown). Notably, CTRP3 mRNA and protein expression levels were highest in the colon, intermediate in the terminal ileum, and

*Current affiliation: Division of Gastroenterology, Department of Medicine, Union Hospital, Tongji Medical College "Huazhong University of Science and Technology," Wuhan, China; §Current affiliation: Department of Pathology, University of South Alabama, Mobile, Alabama
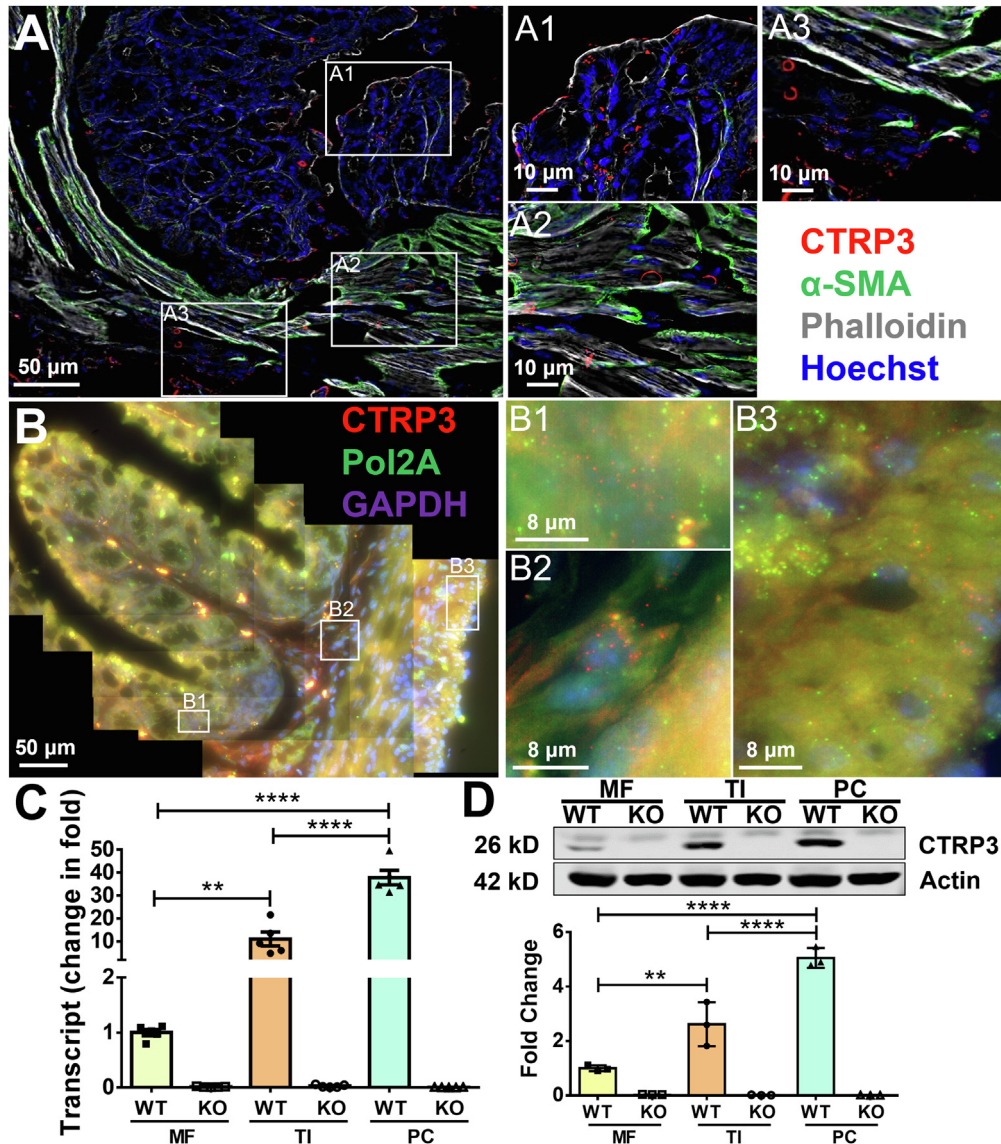
Most current article

Figure 1. CTRP3 is expressed in mouse intestinal epithelial cells, intestinal smooth muscle cells, and mesenteric fat.
(A) Immunofluorescence staining of WT colonic tissue showed that CTRP3 protein was expressed in intestinal epithelial cells (A1), intestinal smooth muscle cells (A2), and mesenteric fat (A3) attached to the colon. α-SMA (smooth muscle actin), Phalloidin (F-actin), and Hoechst (nuclei). (B) Single-molecule RNA fluorescence *in situ* hybridization (smFISH) of WT colonic tissue showed that CTRP3 mRNA (*red dots*) was expressed in intestinal epithelial cells (B1), intestinal smooth muscle cells (B2), and mesenteric fat (B3). Glyceraldehyde 3-phosphate dehydrogenase mRNA (*purple dots*) and RNA polymerase II subunit A (*green dots*) were positive controls. (C) RT-qPCR analysis of CTRP3 mRNA expression levels in the mesenteric fat (MF), terminal ileum (TI), and proximal colon (PC) from CTRP3 KO and WT mice. Signals were normalized to MF of WT mice. Results represented values from 6 mice in 3 independent experiments. (D) Western blot detection and quantification of CTRP3 protein levels in the MF, TI, and PC from CTRP3 KO and WT mice. Protein bands were quantified using ImageJ and normalized to β-actin as an internal control. Signals were then normalized to MF of WT mice. Results are shown as means ± SEM; n = 3 mice/group in *D*. **$P < .01$; and **** $P < .0001$ (1-way analysis of variance).

lowest in the mesenteric fat (Figure 1*C* and *D*). In our studies described here, we focused on the role of CTRP3 in intestinal inflammation.

Deletion of CTRP3 Aggravates Intestinal Inflammation in DSS–Induced Acute Colitis Models

To elucidate the function of CTRP3 in intestinal inflammation *in vivo*, we established a DSS-induced acute colitis model in CTRP3 KO mice and their corresponding WT littermates. The CTRP3 KO mice were born at the expected mendelian ratio, and were viable, fertile, and developed normally with no gross abnormal phenotype under basal conditions.[30] Four different concentrations of DSS (1.2%, 1.5%, 2.0%, and 2.5%) in drinking water were administered to CTRP3 KO and WT mice for 6–10 consecutive days, with 1.2% DSS treatment resulting in the most distinguishable colitis phenotypes between CTRP3 KO and WT mice. DSS of 1.2% was therefore

used in subsequent experiments (Figure 2*A*). After 7 days of 1.2% DSS treatment, CTRP3 KO and WT mice developed obvious colitis, whereas the corresponding water-treated CTRP3 KO and WT mice showed no signs of colitis. Compared with the DSS-treated WT mice, DSS-treated CTRP3 KO mice developed more severe colitis, as evidenced by more pronounced weight loss (Figure 2*B*), higher colitis disease scores based on the evaluation of body weight change, stool consistency, and rectal bleeding[51] (Figure 2*C*), and a lower survival rate (Figure 2*D*). Histologic analysis of the proximal and distal colon revealed more tissue damage and inflammatory cell infiltrates in DSS-treated CTRP3 KO mice than in DSS-treated WT mice (Figure 2*F* and *G*). In addition, the colons of DSS-treated KO mice were significantly shorter than those of DSS-treated WT mice (Figure 2*E*; 5.45 ± 0.16 cm vs 6.56 ± 0.28 cm; $P < .05$).

Under basal conditions (water treatment), CTRP3 KO and WT mice showed no difference in clinical colitis phenotypes (Figure 2*B* and *C*), and histologic analysis likewise revealed no meaningful differences (Figure 2*F* and *G*). However, the colons of water-treated CTRP3 KO mice were significantly shorter than those of WT littermates (Figure 2*E*; 7.48 ± 0.40 cm vs 8.93 ± 0.24 cm; $P < .01$), a phenotype not previously reported. The clinical colitis phenotypes of female CTRP3 KO mice were similar to those of male CTRP3 KO mice.

Overexpression of CTRP3 Attenuates Intestinal Inflammation in DSS–Induced Acute Colitis Models

To further confirm the anti-inflammatory function of CTRP3 in intestinal inflammation, we developed a DSS-induced acute colitis model in CTRP3 overexpressing Tg mice and their corresponding WT littermates. The CTRP3 Tg mice were viable, fertile, and did not display any gross phenotype under baseline conditions.[28] Several concentrations of DSS (1.5%, 2.0%, and 2.5%) in drinking water were administered for 6–10 days. We found that 2% DSS treatment best distinguished the colitis phenotypes between CTRP3 Tg and WT mice (Figure 3*A*). After 7 days of 2% DSS treatment, CTRP3 Tg mice developed significantly less severe colitis than DSS-treated WT mice, experiencing less pronounced weight loss (Figure 3*B*), lower colitis disease scores (Figure 3*C*), and a higher survival rate (Figure 3*D*). Histologic analysis of the proximal and distal colon showed that DSS-treated CTRP3 Tg mice exhibited significantly less tissue damage and fewer inflammatory cell infiltrates than their WT littermates (Figure 3*F* and *G*). Furthermore, the colons of DSS-treated CTRP3 Tg mice were significantly longer than those of their DSS-treated WT littermates (Figure 3*E*; 8.42 ± 0.08 cm vs 7.71 ± 1.05 cm; $P < .001$).

The effects of CTRP3 overexpression under basal conditions were largely inverse to those of CTRP3 deletion. That is, water-treated CTRP3 Tg and WT mice showed no differences in clinical colitis phenotypes (Figure 3*B* and *C*), nor did histologic analysis reveal meaningful differences (Figure 3*F* and *G*), but the colons of water-treated CTRP3 Tg mice were significantly longer than those of WT littermates (Figure 3*E*; 9.72 ± 0.09 cm vs 9.06 ± 0.07 cm; $P < .05$).

Similarly, the clinical colitis phenotypes of female CTRP3 Tg mice were similar to those of male CTRP3 Tg mice.

Thus, CTRP3 expression levels were positively correlated with mouse colon length in basal (water treatment) and colitis (DSS treatment) conditions in CTPR KO and Tg mice, compared with their corresponding WT littermates.

Deletion of CTRP3 Reduces Intestinal SIRT1 and Upregulates Phosphorylated/Acetylated NF-κB p65 and Proinflammatory Cytokines in DSS–Induced Acute Colitis Models

The SIRT1/NF-κB signaling complex is known to influence intestinal inflammation in IBD.[45-47] To evaluate whether CTRP3 attenuates intestinal inflammation through SIRT1/NF-κB signaling, we compared the colonic expression levels of CTRP3, SIRT1, phosphorylated/acetylated NF-κB p65, and proinflammatory cytokines (TNF-α and IL-6) in CTRP3 KO and WT mice after DSS and water treatment. As expected, colonic CTRP3 levels were undetectable in water- and DSS-treated CTRP3 KO mice (Figure 4*A*, *E*, and *F*). Seven days of DSS treatment resulted in a significant reduction of CTRP3 levels in WT mouse colons (Figure 4*A*, *E*, and *F*). Consistent with previous murine studies,[48-50] SIRT1 mRNA and protein levels were reduced in the colonic tissue of the DSS-treated WT mice compared with water-treated WT mice (Figure 4*B*, *E*, and *F*). Compared with WT mice, SIRT1 mRNA and protein levels were lower in CTRP3 KO mice in both water- and DSS-treated groups (Figure 4*B*, *E*, and *F*). NF-κB p65 levels were similar in the colonic tissue of all 4 groups; however, phosphorylated NF-κB p65 levels were significantly higher in CTRP3 KO mice relative to WT mice in water- and DSS-treated groups, respectively (Figure 4*E* and *F*). Acetylated NF-κB p65 levels were higher in CTRP3 KO mice relative to WT mice in the DSS, but not in water-treated groups (Figure 4*E* and *F*). As expected, colonic mRNA levels of TNF-α and IL-6 were upregulated after DSS treatment in WT and CTRP3 KO mice (Figure 4*C* and *D*). In water- and DSS-treated groups, CTRP3 KO mice had upregulated mRNA levels of TNF-α and IL-6 relative to WT mice in the colonic tissue (Figure 4*C* and *D*).

In sum, in an acute colitis model (DSS treatment), compared with WT mice, CTRP3 KO mice had decreased colonic levels of SIRT1 and increased levels of phosphorylated/acetylated NF-κB p65, along with increased TNF-α and IL-6. Under basal conditions (water treatment), CTRP3 KO mice exhibited a similar change compared with WT mice except that acetylated NF-κB p65 did not increase in CTRP3 KO mice (Figure 4*E* and *F*). These data are consistent with the hypothesis that CTRP3 exerts its anti-inflammatory effect in acute colitis mouse models through SIRT1/NF-κB signaling.

Overexpression of CTRP3 Increases Intestinal SIRT1 and Downregulates Phosphorylated/Acetylated NF-κB p65 and Proinflammatory Cytokines in DSS–Induced Acute Colitis Models

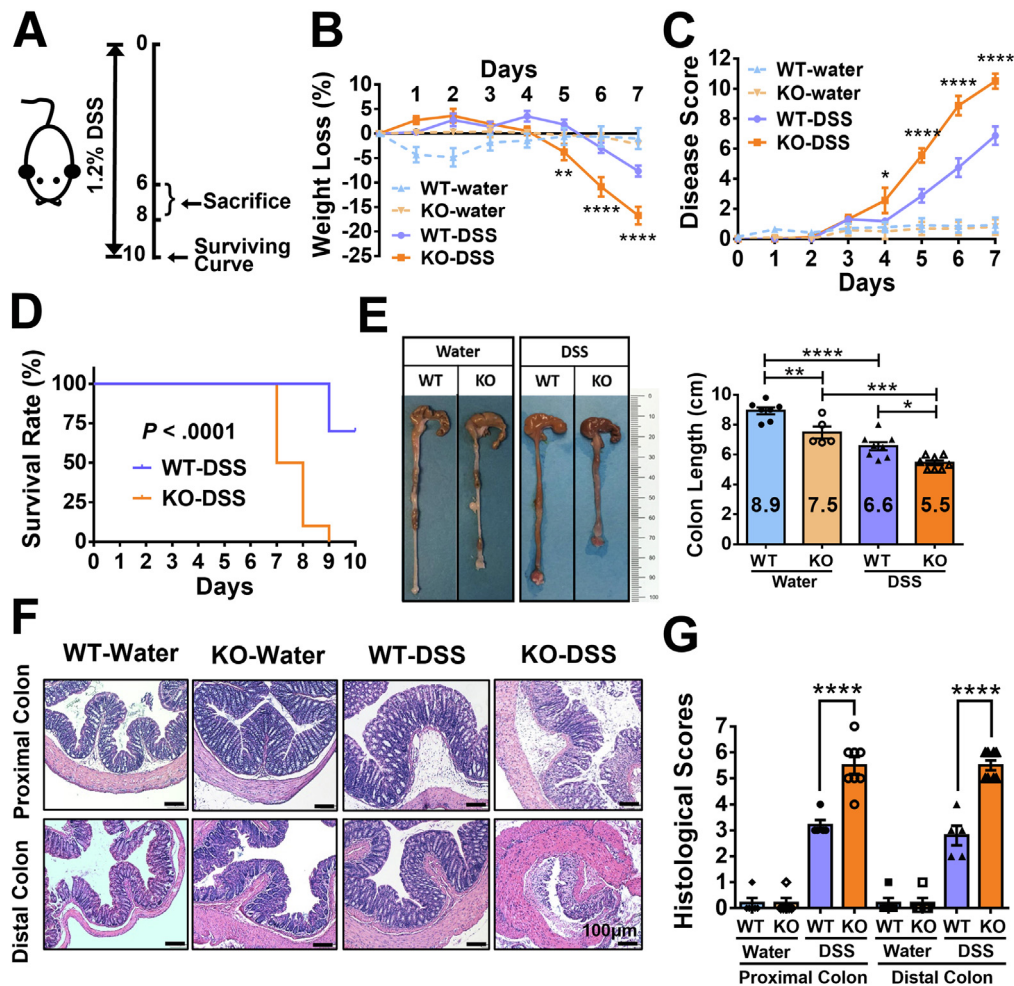To further investigate whether CTRP3 may attenuate intestinal inflammation through SIRT1/NF-κB signaling, we

Figure 2. **CTRP3 KO mice develop more severe colitis than WT littermates in DSS-induced acute colitis models.** (*A*) Experimental scheme for DSS-induced acute colitis in CTRP3 KO and WT mice. DSS of 1.2% was administered in drinking water for 6–10 consecutive days to induce acute colitis. (*B* and *C*) DSS-treated CTRP3 KO mice had more pronounced weight loss and developed more severe colitis phenotypes relative to DSS-treated WT mice. Water-treated CTRP3 KO and WT mice showed no difference in weight loss and colitis phenotypes. Statistical comparison was between DSS-treated CTRP3 KO and WT mice. (*D*) DSS-treated CTRP3 KO mice displayed a lower survival rate relative to DSS-treated WT mice. Log-rank Mantel-Cox test was used for survival analysis. (*E*) The colons of CTRP3 KO mice were significantly shorter than those of WT mice in water- and DSS-treated groups. (*F* and *G*) Hematoxylin and eosin staining of proximal and distal colon revealed more tissue damage and inflammatory cell infiltrates in DSS-treated CTRP3 KO mice than in DSS-treated WT mice. The histologic scores were not different between water-treated CTRP3 KO and WT mice. Scale bar: 100 μm. Results are shown as means $\pm$ SEM; n = 5–10 mice/group. *$P < .05$; **$P < .01$; ***$P < .001$; **** $P < .0001$ (one-way analysis of variance except for the survival curve). The above data were from male CTRP3 KO and WT mice. Female mice had similar clinical phenotypes.

performed similar experiments in water- and DSS-treated CTRP3 overexpressing Tg and WT mice. As anticipated, in water- and DSS-treated CTRP3 Tg mice, colonic CTRP3 levels were significantly higher relative to WT mice (Figure 5*A*, *E*, and *F*). Once again, 7 days of DSS treatment correlated with a significant reduction in CTRP3 levels in WT and CTRP3 Tg mouse colons (Figure 5*A*, *E*, and *F*). Compared with WT mice, SIRT1 mRNA and protein levels were higher in CTRP3 Tg mice in water- and DSS-treated groups (Figure 5*B*, *E*, and *F*). As in our CTRP3 KO mice experiments, NF-κB p65 levels had no show of statistical significance in the colonic tissue among 4 groups (Figure 5*E* and *F*), and phosphorylated/acetylated NF-κB p65 levels were upregulated after DSS treatment. In the DSS-treated

groups, CTRP3 Tg mice had lower phosphorylated/acetylated NF-κB p65 levels compared with WT mice. As expected, colonic mRNA levels of TNF-α and IL-6 were upregulated after DSS treatment in WT and CTRP3 Tg mice (Figure 5*C* and *D*). In DSS-treated (but not water-treated) groups, CTRP3 Tg mice had significantly downregulated colonic mRNA levels of TNF-α and IL-6 relative to WT mice (Figure 5*C* and *D*).

The results of our mechanistic experiments in CTRP3 Tg mice were largely inverse to those conducted in their CTRP3 KO counterparts. In DSS-induced acute colitis models, CTRP3 overexpression correlated with increased SIRT1 and decreased phosphorylated/acetylated NF-κB p65, and was associated with decreased proinflammatory cytokines in the
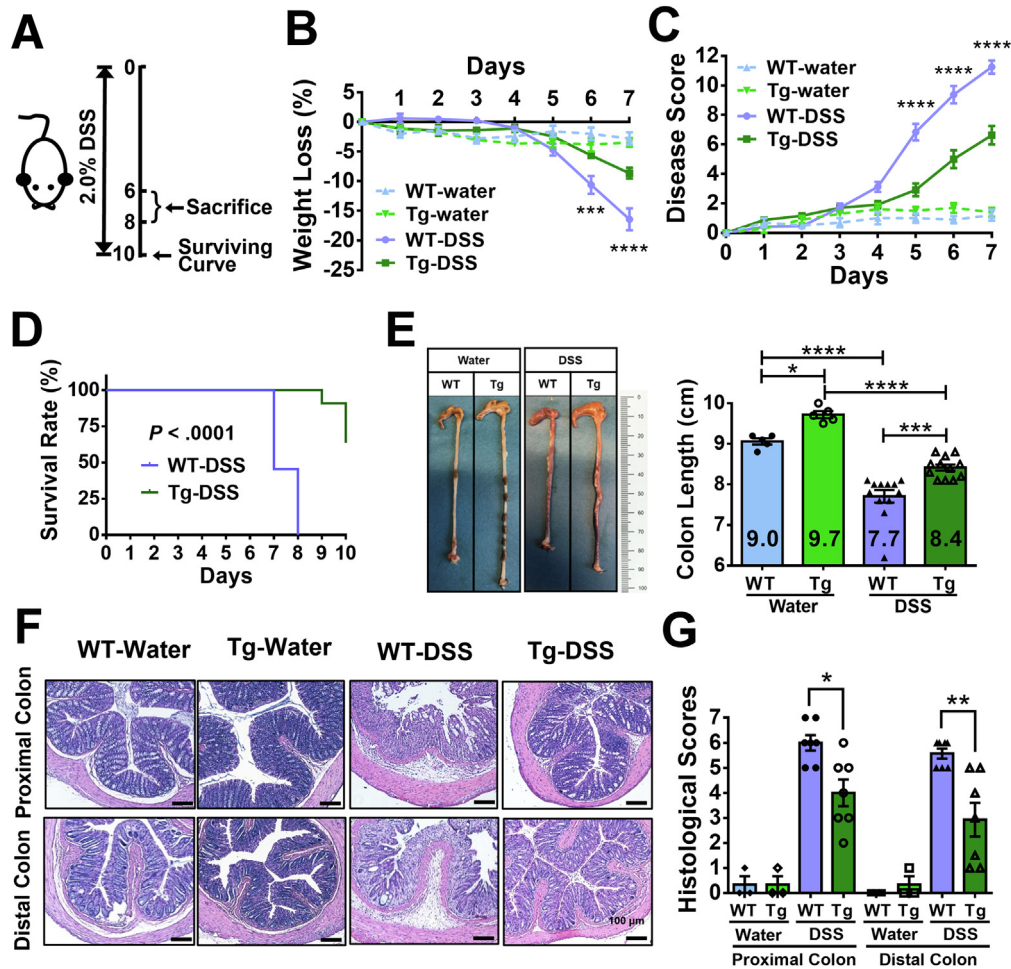
Figure 3. CTRP3 overexpressing Tg mice develop less severe colitis than WT littermates in DSS-induced acute colitis models. (*A*) Experimental scheme for DSS-induced acute colitis in CTRP3 Tg and WT mice. DSS of 2% was administered in drinking water for 6–10 consecutive days to induce acute colitis. (*B* and *C*) DSS-treated CTRP3 Tg mice had less pronounced weight loss and developed less severe colitis relative to DSS-treated WT mice. Water-treated CTRP3 Tg and WT mice exhibited similar weight loss and colitis phenotypes. Statistical comparison was between DSS-treated CTRP3 Tg and WT mice. (*D*) DSS-treated CTRP3 Tg mice displayed a higher survival rate relative to DSS-treated WT littermates. Log-rank Mantel-Cox test was used for survival analysis. (*E*) The colons of CTRP3 Tg mice were significantly longer than those of WT littermates in water- and DSS-treated groups. (*F* and *G*) Hematoxylin and eosin staining of proximal and distal colon revealed less tissue damage and inflammatory cell infiltrates in DSS-treated CTRP3 Tg mice than in DSS-treated WT mice. The histologic scores were not different between water-treated CTRP3 Tg and WT mice. Scale bar: 100 μm. Results are shown as means $\pm$ SEM; n = 5–12 mice/group. $*P < .05$; $**P < .01$; $***P < .001$; $**** P < .0001$ (one-way analysis of variance except for the survival curve). The above data are from male CTRP3 Tg and WT mice; female mice had similar clinical phenotypes.

colons. However, under basal conditions (water treatment), CTRP3 overexpression correlated only with increased SIRT1 levels, but not phosphorylated/acetylated NF-κB p65 or proinflammatory cytokines in the colons. Taken together, our data from CTRP3 KO and Tg mice suggest that CTRP3 may attenuate intestinal inflammation through SIRT1/NF-κB signaling.

CTRP3 Regulates NF-κB p65 Signaling Via SIRT1 in Mouse Intestinal Organoids Derived from CTRP3 KO and Tg Mice

To further investigate whether SIRT1 is the downstream effector of CTRP3 in intestinal inflammation, we generated

three-dimensional intestinal organoids from the distal colons of CTRP3 KO and Tg mice. Two-dimensional intestinal monolayers on Transwell filters were then developed (150 μL media added in the apical chamber and 600 μL media added in the basolateral chamber). Confluent monolayers were differentiated for 24 hours before treatment as follows: CTRP3 KO organoids were treated with a SIRT1 activator (resveratrol, 100 μM) and CTRP3 Tg organoids were treated with a specific SIRT1 inhibitor (Ex-527, 50 μM). Dimethyl sulfoxide (DMSO) was used for vehicle control groups. The monolayers and apical and basolateral culture media were collected after 24 hours of treatment.

We first determined whether the addition of SIRT1 activator resveratrol to CTRP3 KO organoids could restore
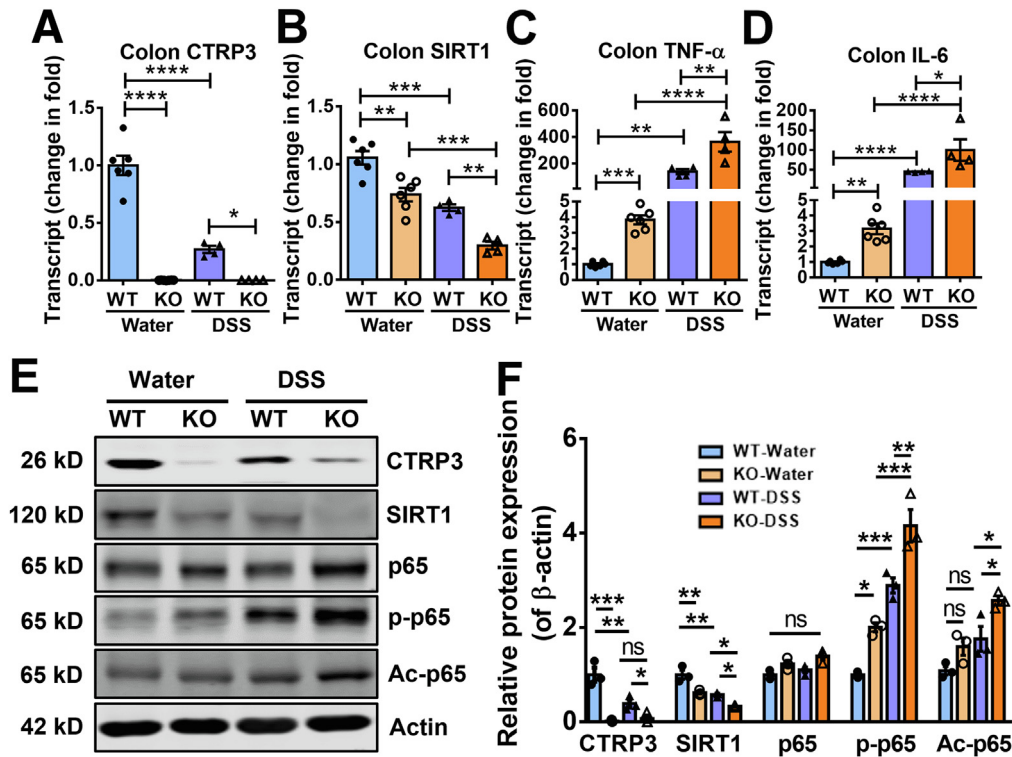
Figure 4. CTRP3 KO mice exhibit decreased intestinal SIRT1 and increased NF-κB p65 transcriptional activity in DSS-induced acute colitis models. (*A*) CTRP3 mRNA levels were reduced in the colons of WT mice after 7 days of 1.2% DSS administration. (*B*) SIRT1 mRNA levels were reduced in the colons of water-treated CTRP3 KO mice relative to those of WT mice. DSS treatment further reduced SIRT1 mRNA levels in the colons of CTRP3 KO mice and WT mice, more severely in CTRP3 KO mice than WT mice. (*C* and *D*) mRNA levels of TNF-α and IL-6 were higher in CTRP3 KO mice compared with WT mice in DSS- and water-treated groups. (*E* and *F*) Western blot detection and quantification of related proteins. The protein bands were quantified using ImageJ and normalized to β-actin (*F*). Results are shown as means ± SEM; n = 4–6 mice/group in *A–D* and n = 3 mice/group in *E* and *F*. *$P < .05$; **$P < .01$; ***$P < .001$; and **** $P < .0001$ (one-way analysis of variance).

the anti-inflammatory effects of CTRP3. SIRT1 levels were lower in the KO-DMSO group compared with the WT-DMSO group. Consistent with our *in vivo* CTRP3 KO mice experiments, NF-κB p65 levels were similar among 4 groups, whereas phosphorylated/acetylated NF-κB p65 levels were upregulated in the KO-DMSO group compared with the WT-DMSO group (Figure 6*A* and *B*). After the addition of resveratrol, SIRT1 levels were increased in KO-resveratrol and WT-resveratrol groups, whereas phosphorylated/acetylated NF-κB p65 levels were significantly downregulated in the KO-resveratrol group, but not in the WT-resveratrol group (Figure 6*A* and *B*). In the apical media, TNF-α and IL-6 levels were similar across all 4 groups. In the basolateral media, TNF-α and IL-6 levels were significantly elevated in the KO-DMSO group compared with the WT-DMSO group, and reduced in the KO-resveratrol group, but not the WT-resveratrol (Figure 6*C* and *D*). These results suggest that the deletion of CTRP3 results in reduced SIRT1 levels and upregulated NF-κB p65 activity and proinflammatory cytokines; and that the addition of a SIRT1 activator can restore the anti-inflammatory effects of CTRP3 by suppressing NF-κB p65 activity and proinflammatory cytokines levels.

We then determined whether the addition of SIRT1 inhibitor Ex-527 to CTRP3 Tg organoids could reverse the anti-inflammatory effects of CTRP3. As expected, CTRP3 and SIRT1 protein levels were significantly elevated in the Tg-DMSO group relative to the WT-DMSO group. After the addition of Ex-527, CTRP3 levels were largely unchanged in both Tg and WT groups, whereas SIRT1 levels were significantly reduced in Tg-Ex-527 and WT-Ex-527 groups compared with Tg-DMSO and WT-DMSO, respectively. The addition of Ex-527 upregulated phosphorylated/acetylated NF-κB p65 levels in the Tg groups (Tg-DMSO vs Tg-Ex-527) (Figure 6*E* and *F*). In the apical media, TNF-α and IL-6 levels were lower in the Tg groups relative to the WT groups (DMSO and Ex-527). In the basolateral media, TNF-α and IL-6 levels were similar between the Tg-DMSO and the WT-DMSO groups. Addition of Ex-527 increased TNF-α and IL-6 levels in the WT-Ex-527 group compared with WT-DMSO, but not in the Tg-Ex-527 group compared with Tg-DMSO (Figure 6*G* and *H*). These findings suggest that CTRP3 modulates downstream SIRT1, thereby suppressing NF-κB signaling and reducing inflammatory cytokine synthesis, ultimately attenuating intestinal inflammation.
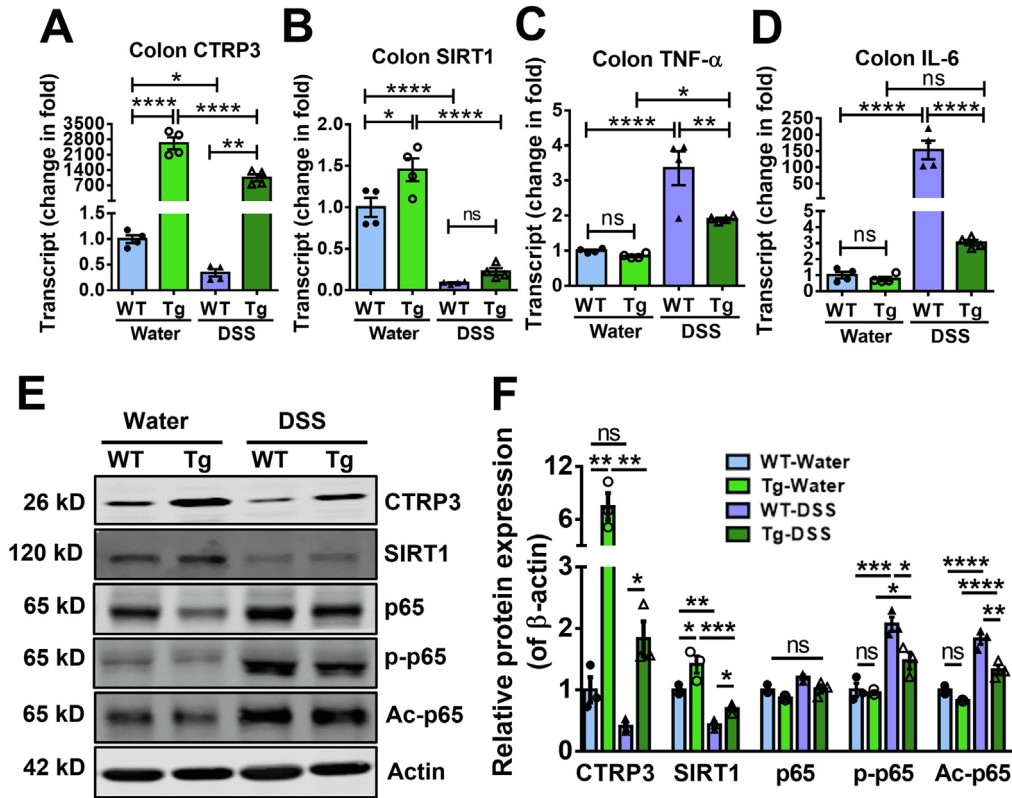
Figure 5. CTRP3 Tg mice exhibit increased intestinal SIRT1 and decreased NF-κB p65 transcriptional activity in DSS-induced acute colitis models. (*A*) CTRP3 mRNA levels were significantly reduced in the colons of CTRP3 Tg and WT mice after 7 days of 2% DSS administration. (*B*) SIRT1 mRNA levels were higher in water-treated CTRP3 Tg mice than in WT mice. DSS treatment reduced SIRT1 mRNA in both CTRP3 Tg and WT mice. (*C* and *D*) mRNA levels of TNF-α and IL-6 were lower in CTRP3 Tg mice compared with WT mice after DSS treatment. (*E* and *F*) Western blot detection and quantification of related proteins. The protein bands were quantified using ImageJ and normalized to β-actin (*F*). Colons were used in all experiments. Results are shown as means ± SEM; n = 4 mice/group in *A–D* and n = 3 mice/group in *E* and *F*. *$P < .05$; **$P < .01$; ***$P < .001$; **** $P < .0001$; ns, not significant (one-way analysis of variance).

Inflamed Intestinal Mucosa from Patients with IBD Expresses Reduced CTRP3 and SIRT1 and Upregulated Phosphorylated/Acetylated NF-κB p65

We next examined whether patients with IBD exhibit the CTRP3/SIRT1/NF-κB correlations observed in our murine studies. Colonic mucosa was obtained from the ascending colon and grouped based on histologic reports as follows: active UC (n = 5) and healthy control subjects (n = 8). CTRP3 and SIRT1 mRNA and protein levels were reduced in the active UC group relative to the control group (Figure 7*A*, *B*, *E*, and *F*). NF-κB p65 levels were similar in both groups; however, phosphorylated and acetylated NF-κB p65 levels were significantly higher in the active UC group relative to the control group (Figure 7*E* and *F*). As expected, colonic mRNA levels of TNF-α and IL-6 were upregulated in the active UC group (Figure 7*C* and *D*).

Similarly, we also obtained 3 types of terminal ileal mucosa from patients with CD who underwent endoscopic or surgical procedures and grouped them based on histologic reports as follows: (1) disease-affected mucosa with discernable ulcers/erosions from patients with CD (active; n = 8); (2) normal-appearing mucosa from the same patients with CD (inactive; n = 8); and (3) normal-appearing mucosa from control patients (control, normal histology; n = 9). The terminal ileum was chosen because it is the most commonly affected intestinal segment to develop creeping fat in CD.[52]

Immunofluorescence staining of the terminal ileal mucosa showed that CTRP3 protein levels were substantially reduced in patients with active CD relative to control patients (Figure 8*A*-*C*). Reverse-transcription quantitative polymerase chain reaction (RT-qPCR) analysis of terminal ileal mucosa showed that mRNA levels of CTRP3 and SIRT1 were reduced in the active and inactive CD groups compared with the control groups (Figure 8*D*). The difference in mRNA levels of CTRP3 and SIRT1 between the inactive and active CD groups was not statistically significant (Figure 8*D*). Protein levels of CTRP3 and SIRT1 in terminal ileal mucosa were likewise reduced in both inactive and active CD groups relative to the control group, again with no statistically significant difference found between the active and inactive groups
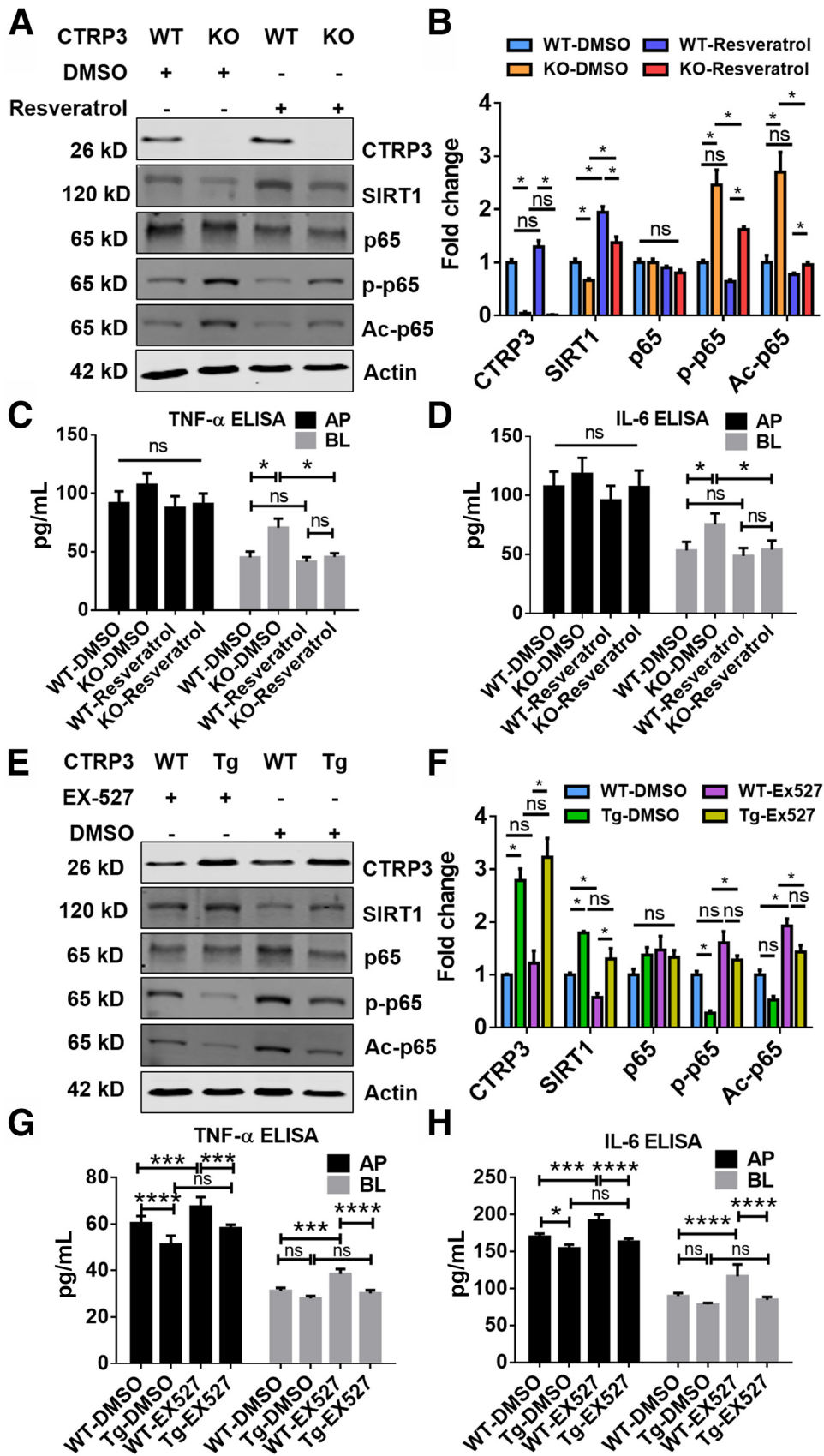
Figure 6. CTRP3 regulates NF-κB p65 signaling via SIRT1 in mouse intestinal organoids derived from CTRP3 KO and Tg mice. (*A* and *B*) After incubation with SIRT1 activator resveratrol (100 μM) for 24 hours, SIRT1 levels were increased in both KO and WT groups, whereas phosphorylated/acetylated NF-κB p65 levels were significantly downregulated in the KO groups but not in the WT groups. (*C* and *D*) TNF-α and IL-6 levels were similar in the apical media across all 4 groups. In contrast, in the basolateral media, TNF-α and IL-6 levels were elevated in the KO-DMSO group compared with the WT-DMSO group, but similar after incubation with SIRT1 activator resveratrol for 24 hours. (*E* and *F*) After incubation with SIRT1 inhibitor Ex-527 (50 μM) for 24 hours, CTRP3 and SIRT1 protein levels were significantly elevated in the Tg intestinal organoids relative to WT intestinal organoids. The addition of SIRT1 inhibitor Ex-527 upregulated the phosphorylated/acetylated NF-κB p65 levels in both KO and WT groups. (*G* and *H*) TNF-α and IL-6 levels were lower in the apical media of Tg groups relative to WT groups (DMSO and Ex-527). In the basolateral media, TNF-α and IL-6 levels were similar between the WT-DMSO group and the Tg-DMSO group, but increased in the WT-Ex-527 group, but not in the Tg- Ex-527 group. Results are shown as means ± SEM; n = 2–3 wells/group for immunoblotting and n = 6–9 wells/group for Elisa. *P < .05; ***P < .001; ****P < .0001; ns, not significant (one-way analysis of variance).
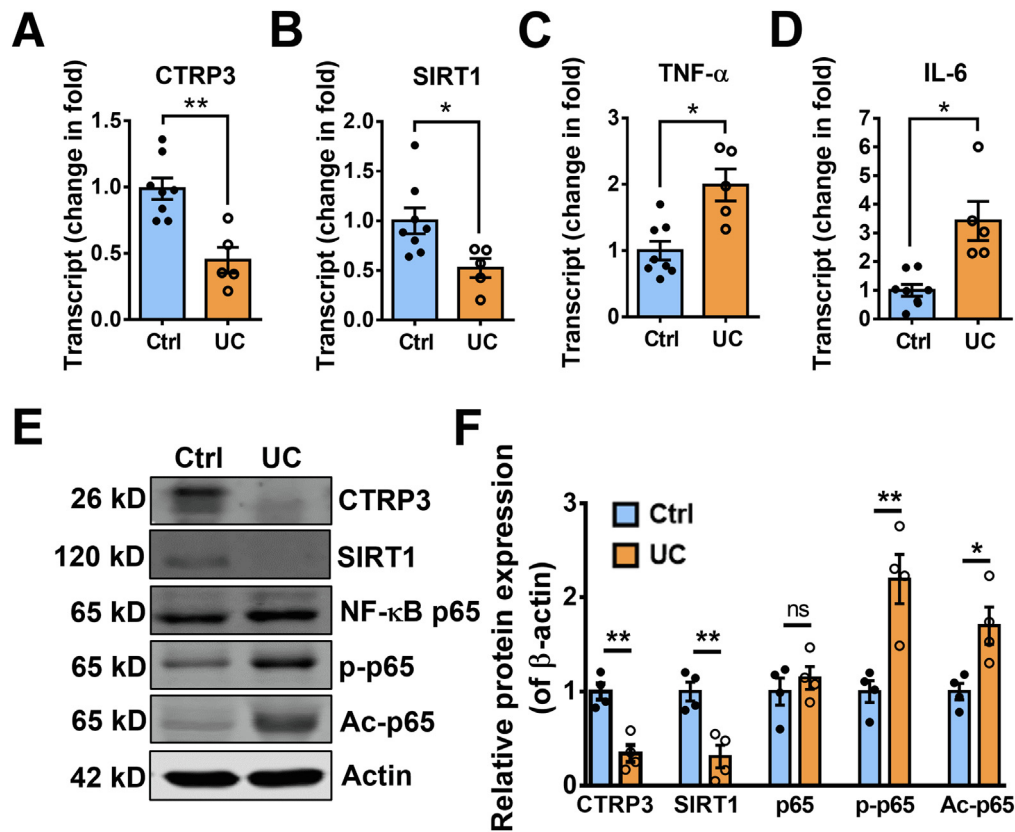
Figure 7. Inflamed colonic mucosa from patients with UC expresses reduced CTRP3 and SIRT1 and upregulated phosphorylated/acetylated NF-κB p65. (*A* and *B*) mRNA levels of CTRP3 and SIRT1 were significantly lower in the colonic mucosa of ascending colon from patients with active UC compared with control patients. The UC group was normalized to the control group. (*C* and *D*) mRNA levels of TNF-α and IL-6 were higher in the colonic mucosa of ascending colon from patients with active UC compared with control patients. (*E* and *F*) Western blot detection and quantification of related proteins. The protein bands were quantified using ImageJ and normalized to β-actin (*F*). Results are shown as means ± SEM; n = 5 for active UC and n = 8 for control subjects in *A–D*; n = 4 patients/group in *E* and *F*. *$P < .05$ and **$P < .01$ (Student *t* test).

(Figure 8*E* and *F*). These results are consistent with a bulk RNA-Seq result by Gettler *et al*[53] which showed lower levels of CTRP3 and SIRT1 in the ileal tissue from the patients with active CD (n = 77) compared with the control subjects (n = 41). Similarly, NF-κB p65 and phosphorylated NF-κB p65 were significantly higher in the active CD groups relative to the control and inactive CD groups (Figure 8*E* and *F*). Again, no statistically significant difference was observed in NF-κB p65 or phosphorylated NF-κB p65 between either the control and inactive groups or the inactive and active CD groups (Figure 8*E* and *F*). Acetylated NF-κB p65 from the terminal ileal mucosa was highest in the active CD group, higher in the inactive CD group, and lowest in the control group (Figure 8*E* and *F*).

Taken together, these data indicate that, compared with control subjects, patients with UC and CD with histologically active inflammation have reduced CTRP3 and SIRT1 and increased phosphorylated/acetylated NF-κB p65 in the intestinal mucosa. These findings are consistent with our murine studies and suggest that CTRP3 may attenuate intestinal inflammation through SIRT1/NF-κB signaling in patients with IBD.

Discussion

Mesenteric fat and its secreted adipokines are increasingly recognized as integral to IBD pathophysiology. Here we report the function of a novel adipokine, CTRP3, in intestinal inflammation. CTRP3 has known anti-inflammatory effects in several inflammatory states (eg, obesity and diabetes) and is found in reduced serum levels among patients with IBD. However, the function of CTRP3 in intestinal inflammation remains unknown. Here, we provide the first *in vivo* evidence that CTRP3 attenuates intestinal inflammation by modeling acute colitis in CTRP3 KO and overexpressing Tg mice. CTRP3 KO mice exhibited more severe colitis, whereas CTRP3 Tg mice exhibited less severe colitis, compared with their corresponding WT littermates, suggesting that CTRP3 is a protective adipokine that suppresses intestinal inflammation.

We offer a putative model that helps to understand the molecular mechanisms through which CTRP3 exerts this anti-inflammatory effect on intestinal inflammation by using *in vivo* complementary KO and Tg mouse colitis models, *ex vivo* mouse intestinal organoid cultures, and human intestinal mucosa from patients with IBD. Our study correlates concurrent reductions of CTRP3 and SIRT1 with upregulated phosphorylated/acetylated NF-κB
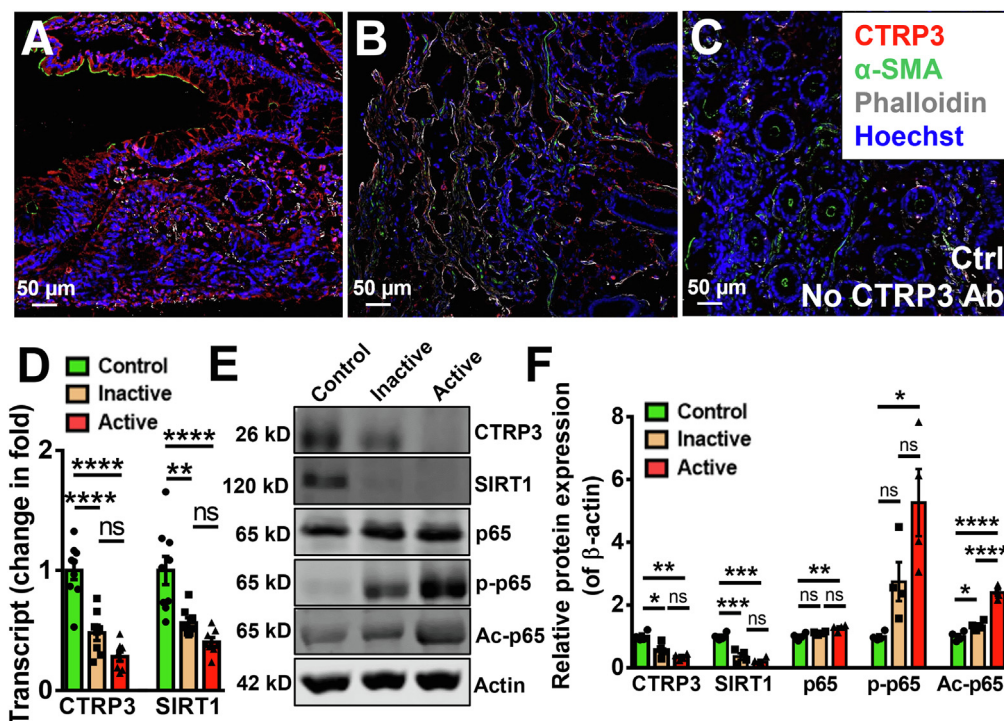
Figure 8. Active inflamed ileal mucosa from patients with CD displays concurrent reductions of CTRP3 and SIRT1 with upregulated NF-κB p65 signaling. (*A–C*) Immunofluorescence staining of human terminal ileal mucosa showed that CTRP3 protein was reduced in the active CD (*B*) compared with normal mucosa (*A*). *C* served as a negative control. α-SMA (smooth muscle actin), Phalloidin (F-actin), and Hoechst (nuclei). (*D*) mRNA levels of CTRP3 and SIRT1 were significantly lower in the terminal ileal mucosa from patients with inactive and active CD (n = 8) compared with control patients (n = 9). No statistically significant differences in both genes were observed between the inactive and active CD groups. Inactive and active epithelial mucosa were obtained from the same 8 patients with CD. Inactive/active groups were normalized to the control group. (*E* and *F*) Western blot detection and quantification of related proteins. The protein bands were quantified using ImageJ and normalized to β-actin. Results are shown as means $\pm$ SEM; n = 8 in active and inactive CD and n = 9 in control subjects in *A–D* and n = 4 patients/group in *E* and *F*. *$P < .05$; **$P < .01$; ***$P < .001$; and ****$P < .0001$ (1-way analysis of variance).

p65 and proinflammatory cytokines TNF-α and IL-6. Although the precise signaling relationship between CTRP3 and SIRT1 remains unknown, the effects of introducing a SIRT1 activator to KO intestinal organoids and a SIRT1 inhibitor to Tg intestinal organoids further suggest that CTRP3 exerts its anti-inflammatory effect in IBD by altering SIRT1 levels and thereby suppressing NF-κB p65 activity.

We also observed that intestinal CTRP3 levels (in addition to serum levels) were reduced in colitis mouse models and patients with IBD. We located the expression of CTRP3 in intestinal epithelial cells, intestinal smooth muscle cells, and mesenteric adipocytes. Although we have not yet established the relative involvement of these cellular sources of CTRP3 in regulating intestinal inflammation, a possible explanation for this finding is that intestinal inflammation causes structural and functional damage to local cellular sources of CTRP3 (or to the most relevant source), resulting in reduced CTRP3 levels, which further exacerbates intestinal inflammation, thus forming a negative feedback loop. Of possible relevance, we found that the difference in the reduction of CTRP3 in patients with active and inactive CD was not statistically significant. This may suggest that the reduced CTRP3 levels are caused by IBD-

related pathophysiological changes other than inflammatory activities.

Our findings also showed that CTRP3 exerts an anti-inflammatory effect even under basal conditions. In the water-treated groups, although CTRP3 KO/Tg mice and corresponding WT littermates had similar clinical phenotypes and intestinal histologic scores, the anti-inflammatory effect of CTRP3 was discernable. First, CTRP3 levels correlated positively with SIRT1 levels and negatively with phosphorylated/acetylated NF-κB p65 transcriptional activity and proinflammatory cytokines in CTRP3 KO mice (no differences observed in CTRP3 Tg mice). Second, CTRP3 levels correlated positively with colon length, which is typically shortened in inflammatory settings. These findings suggest that CTRP3 not only attenuates pathologic intestinal inflammation (DSS treatment in our colitis model), but also preserves an appropriate level of physiological intestinal inflammation (water treatment in our colitis model), that is, the innate immune response of intestinal mucosa to nonpathologic (or prepathologic) aggravation.[54] IBD is increasingly thought to emanate from dysfunction in the innate immune system.[55-58] It is possible that reduced CTRP3 levels in patients with IBD are inadequate to enable the maintenance of homeostatic physiological

inflammation. Future studies will investigate whether and how CTRP3 functions within the innate immune system (in IBD and basal settings). More generally, these findings add to the increasing evidence that adipokines are critical to the maintenance of homeostasis in the intestinal epithelium.[59]

In conclusion, our findings indicate that CTRP3 expression levels correlate negatively with intestinal inflammation in an acute colitis mouse model and in patients with IBD. Furthermore, our findings suggest that CTRP3 attenuates intestinal inflammation through SIRT1/NF-κB signaling to suppress the production of proinflammatory cytokines. Future studies are needed to confirm the precise molecular mechanisms through which CTRP3 activates this signaling, the specific sources of CTRP3 that influence intestinal inflammation, and whether the administration of recombinant CTRP3 and/or SIRT1 activators offers translational potential as a new IBD treatment strategy.

Materials and Methods

CTRP3 Knockout and Overexpressing Transgenic Mice

All animal protocols were approved by the Institutional Animal Care and Use Committee of the Johns Hopkins University School of Medicine. CTRP3 KO (-/-) and overexpressing Tg mouse strains were previously generated.[28,30] CTRP3 KO mice and WT littermates were generated by intercrossing CTRP3 heterozygous (+/-) mice. Littermates were used throughout the study. Male and female mice were examined. All mice were cohoused to control for microbiome differences. On termination of the study, mice were fasted overnight and euthanized and tissues were collected and snap-frozen in liquid nitrogen. Tissues were kept at −80°C until analysis.

Human Samples

Human intestinal epithelial tissue and mesenteric fat were obtained from patients with CD and control patients undergoing endoscopic or surgical procedures through 2 research protocols approved by the Johns Hopkins Institutional Review Boards. Tissue was deidentified, but age, sex, and ethnicity information were noted. Both male and female patients were included. Terminal ileal epithelial tissue was obtained from the following patients: (1) disease-affected mucosa with discernable ulcers/erosions from patients with CD (active; n = 8), (2) normal-appearing mucosa from the same patients with CD (inactive; n = 8), and (3) normal-appearing mucosa from control patients (control, normal histology; n = 9). Ascending colonic epithelial tissue was obtained from patients with UC with active colitis (n = 5) and control patients (n = 8).

Acute DSS-Induced Colitis Mouse Models

Age- and sex-matched CTRP3 KO and Tg mice, along with their WT littermates, were subjected to different concentrations of DSS (1.2%, 1.5%, 2.0%, and 2.5%) in drinking water for 6–10 consecutive days. Mouse body weight, stool consistency, and rectal bleeding were recorded and scored daily as shown in Table 1.[51] Surviving analysis was based on the clinical data collected over 10 days of DSS treatment. On termination of the study, mice were dissected for tissues of interest (mesenteric fat, terminal ileum, and colon). Tissue was fixed in 4% paraformaldehyde overnight followed by paraffin embedding. Paraffin sections 5–8 μm thick were stained with hematoxylin and eosin and examined in a blinded manner by 2 researchers (YF and HY). Tissue damage and inflammatory cell infiltrates were scored as shown in Table 2.[60]

Single-Molecule RNA Fluorescence In Situ Hybridization for RNA Detection in Mouse Intestine

Single-molecule RNA fluorescence *in situ* hybridization uses a probe library consisting of short DNA oligonucleotides labeled with a fluorescent dye that hybridize to a target RNA in fixed cells, allowing RNA quantification and localization at the single-cell level and with single-molecule resolution.[61] All buffers were prepared following RNase precautions and using RNase-free water. Briefly, intestinal tissue was fixed in 4% paraformaldehyde overnight and washed 3 times with phosphate-buffered saline (PBS). The tissue was then embedded in the Optimal Cutting Temperature compound, cut into 5–10 μm frozen sections, and mounted onto collagen-coated coverslips. The sections were washed with 1X PBS and incubated in 70% alcohol overnight at 4°C. After removing 70% alcohol and submerging them in 10% formamide and 2X SSC, they were incubated in prehybridization buffer for 20 minutes. Then, sections were incubated in 50 μL of hybridization solution containing 80 nM DNA probe libraries for mouse CTRP3 (a mixture of 55 cy3-labeled oligonucleotides), mouse RNA polymerase II subunit A (a mixture of 98 cy5-labeled oligonucleotides, a positive control), and mouse glyceraldehyde 3-phosphate dehydrogenase (a mixture of 33 Atto 590–labeled

Table 1. Criteria for the Clinical Disease Score			
	Weight loss	Stool consistency	Rectal bleeding
0	None	Normal	No bleeding
1	1%–5% weight loss	Slight diarrhea	Positive fecal occult blood test (FOBT)
2	5%–10% weight loss	Diarrhea	Slight bleeding
3	10%–15% weight loss	Slight watery diarrhea	Bleeding
4	15%–20% weight loss	Watery diarrhea	Gross bleeding

Table 2. Criteria for the Histologic Score

	Tissue damage	Inflammatory cell infiltration
0	<5%	Infrequent
1	5%–25%	Increased, some neutrophils
2	25%–50%	Submucosal, inflammatory cell clusters
3	50%–75%	Infiltrations muscular
4	>75%	Transmural

oligonucleotides, a positive control) in a humidified chamber overnight at 37°C. After that, sections were rinsed with prewarmed hybridization buffer and incubated for 20 minutes at 37°C. Then, sections were incubated again in the hybridization buffer for 20 minutes at room temperature. Finally, sections were washed with 1X PBS 2 times and mounted on slides with ProLong Diamond Antifade Mountant (Thermo Fisher Scientific). Images were taken and analyzed using an automated inverted Nikon Ti-2 widefield microscope equipped with ×60 1.4NA oil immersion objective lens (Nikon), Spectra X LED light engine (Lumencor), and ORCA-Flash 4.0 V2 sCMOS camera (Hamamatsu).

Immunostaining of Mouse and Human Intestine

Mouse intestinal tissue with attached mesenteric fat or human terminal ileal epithelial tissue was fixed overnight at 4% paraformaldehyde and then embedded in the Optimal Cutting Temperature compound. Tissue staining was performed according to standard immunofluorescence protocols with the following primary antibodies: mouse CTRP3 (generated and provided by GWW, rabbit anti-mouse), human CTRP3 (Invitrogen, PA5-115061, rabbit anti-human), α-SMA-Cy3 (Sigma, A2547), and Phospho-Ezrin (Cell Signaling, #3141). For detection, the following fluorescent-labeled secondary antibodies were used: Alexa Fluor 647 phalloidin (Molecular Probes, A22287), Alexa 488 donkey antirabbit IgG (Molecular Probes, A11008), and Alexa 594 goat antirabbit IgG (Molecular Probes, A11012). The tissue was counterstained using 4′,6-diamidino-2-phenylindole (Sigma, D8417). Images were taken and analyzed using an Olympus IX83 inverted microscope at the Johns Hopkins Ross Fluorescence Imaging Center.

Reverse-Transcription Quantitative Polymerase Chain Reaction

mRNA gene expression of CTRP3, SIRT1, TNF-α, and IL-6 were measured by RT-qPCR. Total RNA of mouse and human intestinal tissue was isolated using the RNeasy Mini Kit (Qiagen) and total RNA of mouse mesenteric fat was isolated using the RNeasy Lipid Tissue Mini Kit (Qiagen). The isolated RNA was transcribed to complementary DNA via Superscript IV VILO Master Mix (Invitrogen). Quantitative PCR was performed with the PowerTrack SYBR Green Master Mix (Thermo Fisher Scientific). All qPCR primers used are listed in Table 3. Data were analyzed by the comparative cycle threshold (Ct) method as means of relative quantitation of gene expression, normalized to an endogenous reference control gene (mouse beta-2-microglobulin or human beta-actin) and relative to a calibrator (normalized Ct value obtained from WT mice or control patients), and expressed as $2^{-\Delta\Delta CT}$.

Western Blot Analysis

Mouse or human intestinal tissue was lysed in 100 μL ice-cold RIPA buffer (Thermo Fisher Scientific) with protease inhibitors (Thermo Fisher Scientific). Homogenates were incubated in a cold room for 2 hours and then centrifuged at 16,000 g for 20 minutes at 4°C. Proteins of the whole-cell extracts of 10–15 μg were separated on 10% sodium dodecyl sulfate polyacrylamide gels for 1 hour at 150 V. Proteins were then transferred to nitrocellulose membranes for 1.5 hours at 100 V. The membranes were blocked with PBS supplemented with 5% dry milk for 1 hour at room temperature, and probed with the following primary antibodies as indicated by each experiment: β-actin (Sigma, A1978), mCTRP3 (provided by GWW), hCTRP3 (Invitrogen, PA5-115061), SIRT1 (Cell Signaling, #2028 and #8469), NF-κB p65 (Santa Cruz, sc-372), p-NF-κB p65 (Cell Signaling, #3033), and Acetyl-NF-κB p65 (Cell Signaling, #3045) at 4°C overnight, and then washed in TBST for 30 minutes. The membranes were probed with corresponding secondary antibodies (IRDye 800CW Goat anti-rabbit IgG, #LI-COR 926-32211 and IRDye 680RD Goat anti-mouse IgG, #LI-COR 926-68070) at 1:10000 dilution for 1 hour at room temperature and the bands were visualized by a Li-Cor Odyssey Fc imaging system and Image Studio software.

Table 3. Primers Information for Reverse-Transcription Quantitative Polymerase Chain Reaction Gene name

	Forward	Reverse
m-B2M	CATGGCTCGCTCGGTGAC	CAGTTCAGTATGTTCGGCTTCC
m-CTRP3	CTTCAGCATGTACAGCTATG	GTTGCCCATTCTTAGCCAGACT
m-TNF-α	CATCTTCTCAAAATTCGAGTGACAA	TGGGAGTAGACAAGGTACAACCC
m-IL-6	CCACTTCACAAGTCGGAGGCTTA	GCAAGTGCATCGTTGTTCATAC
m-SirT1	CCAGACCCTCAAGCCATGTT	CTGTCCGGGATATATTTCCTTTGC
h-actin	GACAGGATGCAGAAGGAGAT	AGTCATAGTCCGCCTAGAAG
h-CTRP3	GAGTCTCCACAAACCGGAGG	TCACCTTTGTCGCCCTTCTC
h-SIRT1	TGCTGGCCTAATAGAGTGGCA	CTCAGCGCCATGGAAAATGT

Signals were quantified using ImageJ (National Institutes of Health, Bethesda, MD) and normalized to β-actin.

Mouse Intestinal Organoid Culture

Mouse intestinal organoids were prepared from the distal colon of male CTRP3 KO and Tg mice (8–12 weeks) as previously described.[62,63] Briefly, mice were euthanized via isoflurane inhalation followed by cervical dislocation, and a portion of the colon ∼2 cm long was removed and bathed in ice-cold PBS with 200 U/mL pen/strep at 4°C for 45 minutes. Isolated crypts obtained after EGTA chelation for 1 hour were embedded in Matrigel (Corning) in 24-well plates (Corning) and culture media was changed every 2 days. Mouse organoids were cultured in 5% CO_2 atmosphere at 37 degrees and passaged via mechanical trituration every 4 days.

Mouse Intestinal Monolayers

Mouse intestinal organoids from passage 5–20 were used to generate monolayers. Briefly, Transwell inserts (polyester membrane with 0.4 μm pore, Corning, 3470) were coated with 200 μg/mL rat tail collagen I (Corning, 354236) and incubated at 37°C overnight. Filters were washed with base-conditioned media without growth factors before plating. Mouse organoids were freed from Matrigel and mechanically triturated before being plated in a precoated Transwell insert with 150 μL media in the apical chamber and 600 μL in the basolateral chamber. Monolayer progression and confluence were monitored by transepithelial electrical resistance (EVOM2 Voltohmmeter, World Precision Instruments). Once the monolayers were confluent as determined via transepithelial electrical resistance over 100 $\Omega \cdot cm^2$, the monolayers were switched to differentiation media. After incubation for 24 hours, the culture media were replaced with differentiation media containing the following medication: 100 μM Resveratrol (Sigma, 34092) for CTRP3 KO groups and 50 μM Ex-527 (Sigma, E7034) for CTRP3 Tg groups. Both medications were prepared in DMSO (Sigma, D8418). Cells and culture media were collected for future analysis after 24 hours of treatment.

Cytokine Enzyme-Linked Immunosorbent Assay

Mouse DuoSet ELISA kits (R&D Systems) were used to measure levels of TNF-α (DY410) and IL-6 (DY406) in the apical and basolateral culture media collected from mouse intestinal organoids following the manufacturer's instructions.

Statistical Analysis

All data presented are representative of 3 or more independent experiments and are shown as mean ± SEM unless stated otherwise. The difference between the 2 groups was assessed by Student t test. The difference among 3 or more groups was compared using one-way or two-way analysis of variance with Tukey multiple comparisons test. Log-rank (Mantel-Cox) testing was used for survival analysis. Statistical analyses were performed using GraphPad Prism software. A statistically significant difference was considered when *$P < .05$, **$P < .01$, ***$P < .001$, and ****$P < .0001$.

References

1. Kaplan GG. The global burden of IBD: from 2015 to 2025. Nat Rev Gastroenterol Hepatol 2015;12:720–727.
2. Dahlhamer JM, Zammitti EP, Ward BW, et al. Prevalence of inflammatory bowel disease among adults aged >/=18 years - United States, 2015. MMWR Morb Mortal Wkly Rep 2016;65:1166–1169.
3. Ye Y, Manne S, Treem WR, et al. Prevalence of inflammatory bowel disease in pediatric and adult populations: recent estimates from large national databases in the United States, 2007-2016. Inflamm Bowel Dis 2020;26:619–625.
4. Chen W, Lu C, Hirota C, et al. Smooth muscle hyperplasia/hypertrophy is the most prominent histological change in Crohn's fibrostenosing bowel strictures: a semiquantitative analysis by using a novel histological grading scheme. J Crohns Colitis 2017;11:92–104.
5. Bettenworth D, Bokemeyer A, Baker M, et al. Assessment of Crohn's disease-associated small bowel strictures and fibrosis on cross-sectional imaging: a systematic review. Gut 2019;68:1115–1126.
6. Yoo JH, Holubar S, Rieder F. Fibrostenotic strictures in Crohn's disease. Intest Res 2020;18:379–401.
7. Rimola J, Capozzi N. Differentiation of fibrotic and inflammatory component of Crohn's disease-associated strictures. Intest Res 2020;18:144–150.
8. Otani S. Pathology of regional enteritis and regional enterocolitis. J Mt Sinai Hosp N Y 1955;22:147–158.
9. Crohn BB, Ginzburg L, Oppenheimer GD. Regional ileitis: a pathologic and clinical entity. 1932. Mt Sinai J Med 2000;67:263–268.
10. Sheehan AL, Warren BF, Gear MW, et al. Fat-wrapping in Crohn's disease: pathological basis and relevance to surgical practice. Br J Surg 1992;79:955–958.
11. Desreumaux P, Ernst O, Geboes K, et al. Inflammatory alterations in mesenteric adipose tissue in Crohn's disease. Gastroenterology 1999;117:73–81.
12. Paul G, Schaffler A, Neumeier M, et al. Profiling adipocytokine secretion from creeping fat in Crohn's disease. Inflamm Bowel Dis 2006;12:471–477.
13. Peyrin-Biroulet L, Chamaillard M, Gonzalez F, et al. Mesenteric fat in Crohn's disease: a pathogenetic hallmark or an innocent bystander? Gut 2007;56:577–583.
14. Coffey JC, O'Leary DP. The mesentery: structure, function, and role in disease. Lancet Gastroenterol Hepatol 2016;1:238–247.
15. Zielinska A, Siwinski P, Sobolewska-Wlodarczyk A, et al. The role of adipose tissue in the pathogenesis of Crohn's disease. Pharmacol Rep 2019;71:105–111.
16. Koon HW, Kim YS, Xu H, et al. Neurotensin induces IL-6 secretion in mouse preadipocytes and adipose tissues during 2,4,6,-trinitrobenzensulphonic acid-induced colitis. Proc Natl Acad Sci U S A 2009;106:8766–8771.
17. Kredel LI, Batra A, Stroh T, et al. Adipokines from local fat cells shape the macrophage compartment of the creeping fat in Crohn's disease. Gut 2013;62:852–862.

18. Scheibe K, Kersten C, Schmied A, et al. Inhibiting interleukin 36 receptor signaling reduces fibrosis in mice with chronic intestinal inflammation. Gastroenterology 2019; 156:1082–1097.

19. Ha CWY, Martin A, Sepich-Poore GD, et al. Translocation of viable gut microbiota to mesenteric adipose drives formation of creeping fat in humans. Cell 2020; 183:666–683.

20. Hofmann C, Chen N, Obermeier F, et al. C1q/TNF-related protein-3 (CTRP-3) is secreted by visceral adipose tissue and exerts antiinflammatory and antifibrotic effects in primary human colonic fibroblasts. Inflamm Bowel Dis 2011;17:2462–2471.

21. Li Y, Wright GL, Peterson JM. C1q/TNF-related protein 3 (CTRP3) function and regulation. Compr Physiol 2017; 7:863–878.

22. Schaffler A, Buechler C. CTRP family: linking immunity to metabolism. Trends Endocrinol Metab 2012;23:194–204.

23. Schaffler A, Scholmerich J, Salzberger B. Adipose tissue as an immunological organ: Toll-like receptors, C1q/TNFs and CTRPs. Trends Immunol 2007;28:393–399.

24. Maeda T, Abe M, Kurisu K, et al. Molecular cloning and characterization of a novel gene, CORS26, encoding a putative secretory protein and its possible involvement in skeletal development. J Biol Chem 2001;276:3628–3634.

25. Wong GW, Wang J, Hug C, et al. A family of Acrp30/adiponectin structural and functional paralogs. Proc Natl Acad Sci U S A 2004;101:10302–10307.

26. Wong GW, Krawczyk SA, Kitidis-Mitrokostas C, et al. Molecular, biochemical and functional characterizations of C1q/TNF family members: adipose-tissue-selective expression patterns, regulation by PPAR-gamma agonist, cysteine-mediated oligomerizations, combinatorial associations and metabolic functions. Biochem J 2008;416:161–177.

27. Petersen PS, Wolf RM, Lei X, et al. Immunomodulatory roles of CTRP3 in endotoxemia and metabolic stress. Physiol Rep 2016;4:e12735.

28. Peterson JM, Seldin MM, Wei Z, et al. CTRP3 attenuates diet-induced hepatic steatosis by regulating triglyceride metabolism. Am J Physiol Gastrointest Liver Physiol 2013;305:G214–224.

29. Peterson JM, Wei Z, Wong GW. C1q/TNF-related protein-3 (CTRP3), a novel adipokine that regulates hepatic glucose output. J Biol Chem 2010; 285:39691–39701.

30. Wolf RM, Lei X, Yang ZC, et al. CTRP3 deficiency reduces liver size and alters IL-6 and TGFbeta levels in obese mice. Am J Physiol Endocrinol Metab 2016; 310:E332–345.

31. Ban B, Bai B, Zhang M, et al. Low serum cartonectin/CTRP3 concentrations in newly diagnosed type 2 diabetes mellitus: in vivo regulation of cartonectin by glucose. PLoS One 2014;9:e112931.

32. Choi KM, Hwang SY, Hong HC, et al. C1q/TNF-related protein-3 (CTRP-3) and pigment epithelium-derived factor (PEDF) concentrations in patients with type 2 diabetes and metabolic syndrome. Diabetes 2012;61:2932–2936.

33. Deng W, Li C, Zhang Y, et al. Serum C1q/TNF-related protein-3 (CTRP3) levels are decreased in obesity and hypertension and are negatively correlated with parameters of insulin resistance. Diabetol Metab Syndr 2015; 7:33.

34. Park HS, Park JY, Yu R. Relationship of obesity and visceral adiposity with serum concentrations of CRP, TNF-alpha and IL-6. Diabetes Res Clin Pract 2005; 69:29–35.

35. Yoo HJ, Hwang SY, Hong HC, et al. Implication of progranulin and C1q/TNF-related protein-3 (CTRP3) on inflammation and atherosclerosis in subjects with or without metabolic syndrome. PLoS One 2013;8:e55744.

36. Wolf RM, Steele KE, Peterson LA, et al. Lower circulating C1q/TNF-related protein-3 (CTRP3) levels are associated with obesity: a cross-sectional study. PLoS One 2015; 10:e0133955.

37. Wagner RM, Sivagnanam K, Clark WA, et al. Divergent relationship of circulating CTRP3 levels between obesity and gender: a cross-sectional study. PeerJ 2016; 4:e2573.

38. Flehmig G, Scholz M, Kloting N, et al. Identification of adipokine clusters related to parameters of fat mass, insulin sensitivity and inflammation. PLoS One 2014;9: e99785.

39. Mohamadinarab M, Ahmadi R, Gholamrezayi A, et al. Serum levels of C1q/TNF-related protein-3 in inflammatory bowel disease patients and its inverse association with inflammatory cytokines and insulin resistance. IUBMB Life 2020;72:1698–1704.

40. Li Y, Ozment T, Wright GL, et al. Identification of putative receptors for the novel adipokine CTRP3 using ligand-receptor capture technology. PLoS One 2016;11: e0164593.

41. Lv C, He Y, Wei M, et al. CTRP3 ameliorates ceruleininduced severe acute pancreatitis in mice via SIRT1/NF-kappaB/p53 axis. Biosci Rep 2020;40:BSR20200092.

42. Murayama MA, Kakuta S, Maruhashi T, et al. CTRP3 plays an important role in the development of collagen-induced arthritis in mice. Biochem Biophys Res Commun 2014;443:42–48.

43. Wu D, Lei H, Wang JY, et al. CTRP3 attenuates post-infarct cardiac fibrosis by targeting Smad3 activation and inhibiting myofibroblast differentiation. J Mol Med (Berl) 2015;93:1311–1325.

44. Yuan YP, Ma ZG, Zhang X, et al. CTRP3 protected against doxorubicin-induced cardiac dysfunction, inflammation and cell death via activation of Sirt1. J Mol Cell Cardiol 2018;114:38–47.

45. Lawrence T. The nuclear factor NF-kappaB pathway in inflammation. Cold Spring Harb Perspect Biol 2009; 1:a001651.

46. Rogler G, Brand K, Vogl D, et al. Nuclear factor kappaB is activated in macrophages and epithelial cells of inflamed intestinal mucosa. Gastroenterology 1998;115:357–369.

47. Schreiber S, Nikolaus S, Hampe J. Activation of nuclear factor kappa B inflammatory bowel disease. Gut 1998; 42:477–484.

48. Wellman AS, Metukuri MR, Kazgan N, et al. Intestinal epithelial sirtuin 1 regulates intestinal inflammation during aging in mice by altering the intestinal microbiota. Gastroenterology 2017;153:772–786.

49. Lo Sasso G, Ryu D, Mouchiroud L, et al. Loss of Sirt1 function improves intestinal anti-bacterial defense and protects from colitis-induced colorectal cancer. PLoS One 2014;9:e102495.

50. Caruso R, Marafini I, Franze E, et al. Defective expression of SIRT1 contributes to sustain inflammatory pathways in the gut. Mucosal Immunol 2014;7:1467–1479.

51. Cooper HS, Murthy SN, Shah RS, et al. Clinicopathologic study of dextran sulfate sodium experimental murine colitis. Lab Invest 1993;69:238–249.

52. Eder P, Adler M, Dobrowolska A, et al. The role of adipose tissue in the pathogenesis and therapeutic outcomes of inflammatory bowel disease. Cells 2019; 8:628.

53. Gettler K, Giri M, Kenigsberg E, et al. Prioritizing Crohn's disease genes by integrating association signals with gene expression implicates monocyte subsets. Genes Immun 2019;20:577–588.

54. Fiocchi C. What is "physiological" intestinal inflammation and how does it differ from "pathological" inflammation? Inflamm Bowel Dis 2008;14(Suppl 2):S77–78.

55. Cho JH. The genetics and immunopathogenesis of inflammatory bowel disease. Nat Rev Immunol 2008; 8:458–466.

56. Geremia A, Biancheri P, Allan P, et al. Innate and adaptive immunity in inflammatory bowel disease. Autoimmun Rev 2014;13:3–10.

57. Mitsialis V, Wall S, Liu P, et al. Single-cell analyses of colon and blood reveal distinct immune cell signatures of ulcerative colitis and Crohn's disease. Gastroenterology 2020;159:591–608.

58. Corridoni D, Chapman T, Ambrose T, et al. Emerging mechanisms of innate immunity and their translational potential in inflammatory bowel disease. Front Med (Lausanne) 2018;5:32.

59. Tsai YW, Fu SH, Dong JL, et al. Adipokine-modulated immunological homeostasis shapes the pathophysiology of inflammatory bowel disease. Int J Mol Sci 2020;21:9564.

60. Koelink PJ, Wildenberg ME, Stitt LW, et al. Development of reliable, valid and responsive scoring systems for endoscopy and histology in animal models for inflammatory bowel disease. J Crohns Colitis 2018;12:794–803.

61. Lyubimova A, Itzkovitz S, Junker JP, et al. Single-molecule mRNA detection and counting in mammalian tissue. Nat Protoc 2013;8:1743–1758.

62. Sato T, Stange DE, Ferrante M, et al. Long-term expansion of epithelial organoids from human colon, adenoma, adenocarcinoma, and Barrett's epithelium. Gastroenterology 2011;141:1762–1772.

63. Johnson K, Yin J, In JG, et al. Cholinergic-induced anion secretion in murine jejunal enteroids involves synergy between muscarinic and nicotinic pathways. Am J Physiol Cell Physiol 2020;319:C321–C330.

Correspondence
Address correspondence to: Huimin Yu, MD, PhD, Johns Hopkins University School of Medicine, 720 Rutland Avenue, Ross Research Building, Room 933, Baltimore, Maryland 21205. e-mail: hyu20@jhmi.edu.